

Coordinated vehicle dispatching and charging scheduling for an electric ride-hailing fleet under charging congestion and dynamic prices

Tai-Yu Ma*, Luxembourg Institute of Socio-Economic Research (LISER), 11 Porte des Sciences, 4366 Esch-sur-Alzette, Luxembourg

Richard D. Connors, Department of Engineering, University of Luxembourg, Esch-sur-Alzette, Luxembourg
Francesco Viti, Department of Engineering, University of Luxembourg, Esch-sur-Alzette, Luxembourg

Abstract

Effective utilization of charging station capacity plays an important role in enhancing the profitability of ride-hailing systems using electric vehicles. Existing studies assume constant energy prices and uncapacitated charging stations or do not explicitly consider vehicle queuing at charging stations, resulting in over-optimistic charging infrastructure utilization. In this study, we develop a dynamic charging scheduling method (named CongestionAware) that anticipates vehicles' energy needs and coordinates their charging operations with real-time energy prices to avoid long waiting time at charging stations and increase the total profit of the system. A sequential mixed integer linear programming model is proposed to devise vehicles' day-ahead charging plans based on their experienced charging waiting times and energy consumption. The obtained charging plans are adapted within the day in response to vehicles' energy needs and charging station congestion. The developed charging policy is tested using NYC yellow taxi data in a Manhattan-like study area with a fleet size of 100 vehicles given the scenarios of 3000 and 4000 customers per day. The computational results show that our CongestionAware policy outperforms different benchmark policies with up to +15.06% profit and +19.16% service rate for 4000 customers per day. Sensitivity analysis is conducted with different system parameters and managerial insights are discussed.

Keywords: ride-hailing, electric vehicle, dynamic charging management, capacitated charging network, time-of-use energy prices, optimization

1. Introduction

The climate change crisis has motivated governments and Transport Network Companies to accelerate fleet electrification to reduce CO₂ emissions. Charging management is becoming a significant issue for deploying this clean air transition policy due to the long charging times of electric vehicles (EVs) compared to refueling internal combustion engine vehicles. According to a recent TLC Electrification Report (Taxi & Limousine Commission, 2022), TLC plans to transform its licensed fleet to EVs by 2030 to reduce environmental impact (around 600k tons of CO₂ in 2022). However, due to the high investment costs of rapid chargers, only a limited number of fast charging stations are available in major cities in the United States. Furthermore, the high daily mileage of TLC's vehicles necessitates drivers to charge their vehicles several times a day, relying mainly on rapid chargers to save charging time (Jenn, 2019). Optimizing the utilization of limited fast-charging resources in a stochastic environment has become a significant challenge for this EV transition.

Several factors make dynamic charging management of electric ride-hailing systems challenging. First, customer demand is volatile, affecting vehicles' charging needs over time. Second, rapid chargers (charging power $\geq 50\text{kWh}$) are limited due to their high investment costs. This might result in EVs queuing at charging stations, thereby increasing charging station search costs for the drivers. Furthermore, charging costs might vary according to the time of day due to variations in electricity prices. The decision on when and how much energy to recharge becomes a significant online decision problem for drivers/fleet operators to maximize their profit. However, most studies assume constant energy prices and neglect congestion issues at charging stations (Al-Kanj et al., 2020; Shi et al., 2020).

Methodologies developed in recent years are mainly based on mixed integer programming optimization approaches, where the problem is decomposed into sequential sub-problems over different planning horizons for vehicle dispatching, relocation, and charging scheduling to respond to uncertain customer demand. In the first stage, a long-time horizon planning model is used to determine how many vehicles to charge and at what type of chargers for each decision time interval (typically half an hour) for the day by anticipating vehicles' energy demand. The objective is to determine vehicles' charging times and durations for the day to minimize a desired objective function (e.g. minimize the number of total charging trips and rejected customers (Jamshidi et al., 2021) or the shortage of available vehicles (Zalesak and Samaranayake, 2021) or total charging operational costs (Ma, 2021) for the planning horizon. In the second stage, a short-time horizon planning model is applied to determine where to charge to minimize total charging access costs or charging operational costs (including access times, waiting times, and charging durations) under the capacity constraints of charging stations. Three drawbacks can be identified in these existing works. First, when vehicles wait to charge at charging stations, there are no maximum waiting time limits, resulting in unrealistically long waiting times at charging stations. Second, there is no minimum charging duration constraint per each charging operation, which might result in undesirably short charging durations (damaging battery lifespan) and inefficient charging operations (requiring higher charging access times/costs and setup times due to more frequent charging operations). Third, vehicles only need enough energy to reach the end of their working day, when overnight charging is available; ignoring this results in more charging than is needed. Consequently, vehicles might charge longer, resulting in a shortage of available vehicles to serve customers.

This study proposes a new sequential mixed integer linear programming (MILP) model by considering more realistic charging operations under congested charging facilities and real-time energy prices for ride-hailing systems using EVs. We propose a day-ahead charging scheduling model by anticipating vehicle waiting times at different chargers and vehicle energy consumption for the day. A reactive model is proposed to adapt the current system state and anticipate vehicles' waiting times. Energy needed to the end of the day is anticipated and vehicle charging time, duration, and where to charge are optimized online. In doing so, the proposed charging policy significantly increases customer service rate and operator's profit due to reducing vehicles' waiting times and charging durations at charging stations. Numerical experiments are conducted using NYC yellow taxi data, and the impacts of different system parameters (battery capacity, maximum waiting times at chargers, and number of chargers) are analyzed. We validate the proposed approach by comparing it with several benchmark charging policies, showing its benefit in increasing the customer's service rate and total profit of the operator.

The organization of this paper is as follows. We first present the related studies. Section 3 presents the problem description, developed models and benchmark charging policies. Section 4 describes the test instances and reports the computational studies. The impact of different system parameters is analyzed. Finally, the conclusion is drawn, and future extensions are discussed.

2. Related studies

Dynamic charging management of ride-hailing systems involves sequential decision making under uncertainty. Recent works for addressing this problem are mainly based on optimization-based approach and reinforcement learning (RL). Earlier studies can be classified into two categories of methodology: sequential mixed integer programming approaches and RL. The first approach decomposes the dynamic charging scheduling problem into multiple decision horizons where the long horizon planning for the day to determine the number of vehicles to charge, charging time, and durations for each charging decision time interval (e.g. half an hour). In contrast, short-horizon planning aims to determine where to charge, given the charging plans obtained at the first step. The second approach (RL) considers dynamic vehicle dispatching, relocation, and charging management as sequential decision-making problems under uncertainty and models the problem as a Markov decision process. Under the RL framework, the operator is considered as an agent making these decisions to maximize the total profit of the system. Recent studies extend the single-agent-based approach to the multi-agent-based approach to allow individual vehicles to make their own decisions in response to local information of the system. More detailed reviews are described as follows.

Optimization-based approaches: Earlier works on dynamic ride-hailing systems focus on vehicle dispatching and relocation optimization under stochastic demand. Vehicle charging operations are simplified by assuming uncapacitated charging stations or simply neglected by considering internal combustion engine vehicles. For example, Zhang et al. (2016) proposed a model predictive control approach for operating a dynamic ride-hailing system using autonomous vehicles. Vehicles' charging scheduling problems are not considered. Iacobucci et al. (2019) extended their work for the fleet management of shared autonomous EVs based on the model predictive control approach. Two different model predictive control schemes interact over different planning horizons: one for vehicle dispatching and relocation decisions and another for vehicle charging scheduling. However, the applicability of the developed approach is limited to small problem sizes with tens of vehicles, and charging congestion is not considered by assuming uncapacitated charging stations. To address more realistic charging congestion scenarios, several studies developed dynamic charging management strategies for dynamic ride-hailing systems. For example, Jamshidi et al. (2021) proposed a three-stage sequential MILP model to address e-taxi dispatching, relocation, and charging with charging station capacity constraints and time-of-use energy prices. However, waiting times at charging stations are approximated without explicitly modeling charging queuing times on different chargers. Zalesak and Samaranayake (2021) developed a MILP model to optimize the charging schedules of ride-pooling systems using EVs. A two-stage planning framework is proposed: a long-time planning horizon optimization model for determining when to charge and a short-time planning horizon optimization model to determine where to charge. The objective of the long-time horizon planning model is to maintain a sufficient fleet size to meet varying customers' demands and vehicles' energy needs for the planning horizon. The number of vehicles recharged for each decision time interval cannot exceed the capacity of total charging stations. Heterogeneous charging infrastructure and time-dependent energy prices are not considered. For the short-time horizon planning, a simple vehicle-to-charging-station assignment model is formulated to minimize vehicles' total charging access distance under charging station capacity constraints. Ma (2021) proposed a two-stage MILP model for dynamic charging management of shared ride-hailing services. The developed approach anticipates vehicles' driving needs and waiting time at chargers to determine charging time and durations per half an hour to minimize total daily charging operational costs. An online vehicle-to-charger assignment model is applied to minimize total charging operational times under charging station capacity constraints. Several simplifications are made for this study. First, the charging speed of vehicles is assumed linear without distinguishing the fact that vehicles' charging speed slows down when their state-of-charge (SoC) is above a threshold (around 80% of vehicles' battery capacity). Second, the charging infrastructure is homogeneous, and the minimum charging duration per charging operation is not considered. Pantelidis et al. (2022) developed a MILP to optimize vehicle relocation and charging for electric carshare systems jointly. The optimization problem is modeled as a route-capacitated minimum cost-flow relocation problem. A node-charge graph is proposed to allow partial recharges over different discretized recharge levels to cover vehicle energy needs for serving customers. A simulation case study is conducted using realistic carshare data in Brooklyn. Yang et al. (2019) proposed a two-stage charging coordination approach for optimizing electric taxi fleet charging operations by considering the current queuing state at charging stations. The first-stage problem determines when vehicles go recharge by a time-dependent charging cost function as an average revenue loss per kWh charged. The second-stage problem determines where to recharge as a Nash equilibrium problem to model non-cooperative taxi drivers' charging station selections. Yi and Smart (2021) proposed a heuristic for vehicle repositioning and charging management of ride-hailing systems using autonomous EVs. Vehicles go to the nearest unoccupied charging stations to recharge when their SoCs are below a predefined threshold. Dean et al. (2022) proposed a MILP model to jointly optimize vehicle relocation and charging operations for shared autonomous EVs using zones as the operational units. When assigning vehicles for charging in a zone, the number of vehicles for charging cannot exceed its total charging station capacity. Vehicles queuing times at charging stations are not explicitly modeled.

Reinforcement-learning-based approaches: RL is a model-free approach that has been successfully applied to solving various sequential decision-making problems under uncertainty (Farazi et al., 2021). For dynamic ride-hailing systems using EVs, Al-Kanj et al. (2020) proposed an approximate dynamic

programming approach for ride-hailing fleet management to maximize the operators' profit. Vehicles' dispatching, relocation, and charging decisions (actions) are controlled by a central controller. The system state (vehicles' locations, SoCs, activities, etc.) and time are discretized. Charging stations are assumed uncapacitated and vehicles are fully recharged for each charging operation. As the possible state-action combination is huge, an approximate dynamic programming approach is applied with hierarchical aggregation for value function approximation. Yan et al. (2023) proposed an online model-based RL algorithm based on State-action-reward-state-action (SARSA) for joint vehicle dispatch and charging optimization of electric ride-hailing systems. Like the previous study, a full-recharge policy is applied. Kullman et al. (2021) developed a deep reinforcement learning (DRL) approach to overcome the curses of dimensionality for electric ride-hailing systems. A hybrid scheme is proposed where the problem of vehicle dispatching is solved by a MILP optimization model, and vehicle relocation and charging decisions are made under the RL framework. Unlike the single-agent-based RL approaches, Ahadi et al. (2022) propose a multiagent-based DRL approach for the fleet management of shared and autonomous EVs. The authors proposed a hierarchical learning and mean-field approximation approach to coordinate vehicles' charging decisions under charging station capacity constraints to maximize the total revenue of the fleet. A comprehensive review of RL-based approaches for EV charging management can be found in Abdullah et al. (2021).

3. Dynamic charging management with charging congestion and real-time energy prices

In this section, we first present the problem description, then formulate the problem using mixed integer linear programming, which includes three models: a) day-ahead charging planning, b) vehicle dispatching, and c) online vehicle-to-charger assignment. We present the simulation framework to test the proposed approach and compare its performance with four benchmark charging approaches.

Notation

T	Daily charging planning horizon (i.e., 24 hours ahead)
H^b	Set of decision epochs for batch dispatch with the decision time interval Δ_b (e.g. 1 minute), i.e., $H^b = \{1, 2, \dots, \lfloor \frac{T-T_0}{\Delta_b} \rfloor\}$ where T_0 is the starting time of service (6:00 a.m.)
H^ℓ	Set of decision epochs for charging schedule planning for the day with decision time interval Δ_ℓ (e.g., 30 minutes), $H^\ell = \{1, 2, \dots, \lfloor \frac{T-T_0}{\Delta_\ell} \rfloor\}$
t	Batch dispatch time index, $t \in H^b$. Note that the clock time is T_0 for $t = 0$.
R_t	Set of unserved requests (customers) at time t
V	Set of vehicles
V_h	Set of idle vehicles at the beginning of decision epoch h
u	Type of chargers, $u \in U = \{\text{fast, slow}\}$
S	Set of chargers
p_h	Average energy price in charging decision epoch h
λ_h	The number of customers' arrivals during charging decision epoch h
C	Average travel cost for recharge per charging operation (dollar)
e_{vh}	Battery level of vehicle v at the beginning of epoch h (Kilowatt-hour, kWh)
φ_s	Charging power of charger s (kW)
μ	Energy consumption rate per kilometer traveled (kWh/km)
γ	Average profit per minute traveled (dollar/km)
α_s	Minimum charging time per charging operation for the charger type for the charger s
B_v	Battery capacity of vehicle v (KWh)
E_v^{min}	Minimum (reserve) SoC of vehicle v (kWh)

E_v^{max}	Maximum threshold of SoC of vehicle v with theoretical maximum charging speed (kWh) (e.g. 80% of vehicle's battery capacity)
E_v^{init}	Initial SoC of vehicle v (KWh) (100% of vehicle's battery capacity)
\bar{E}_v	Planned battery level after recharge for vehicle v at the end of charging decision epoch h (h is dropped)
Y_s^{max}	The maximum amount of energy that can be charged on charger s during one charging decision epoch (kWh)
δ_h	Average energy consumption of a vehicle for decision epoch $h \in H^l$ (kWh)
\bar{t}_{vs}	Travel time from vehicle v 's current location to the location of charger s (minute)
\bar{d}_{ij}	Shortest path distance between location i and j (km)
g_r	Taxi fare for ride request r (dollar)
W_{rt}	Experienced wait time of request r by the time t
W^{max}	Maximum waiting time of customers (same for each customer)
W_{vs}	Waiting (queuing) time at charger s for vehicle v (h is dropped)
\bar{W}_{hs}	Expected waiting time of vehicles when arriving at the charger s at the beginning of epoch h
π	Cost per kilometer traveled of vehicles (dollar)
θ	SoC threshold under which vehicles are added to the pool of go-charge vehicles. Note SoC is measured in percentage of vehicles' battery capacity.

Decision variables

x_{hs}^v	Indicator: 1 if vehicle v is assigned to charger s in epoch h , and 0 otherwise
y_{hs}^v	Amount of charged energy for vehicle v at charger s during epoch h
x_{vs}	Indicator: 1 if a vehicle is assigned to charger s , and 0 otherwise
y_{vs}	Amount of charged energy for vehicle v at charger s
m_{rv}	Indicator: 1 if request r is assigned to vehicle v , and 0 otherwise

3.1. Problem description

Consider a ride-hailing system operated by a transport network company (operator) with a fleet of EVs. Vehicles are equipped with dedicated communication devices for real-time communication to the operator's control center of vehicle states (e.g. location, vehicle's activity, e.g. idled, charging or serving customers, SoCs of vehicles, etc.). Vehicles' dispatching and charging operations are controlled by the operator. Customers arrive randomly and send their ride requests via a smartphone app by indicating their pickup location and desired pickup time. The operator applies a batch assignment method for vehicle dispatching per batch assignment epoch (e.g. 1 minute). Customers have limited patience, which is quantified by a maximum waiting time threshold (assume identical for each customer). Furthermore, we assume customers are engaged to use the service when their waiting time is below the above threshold. We divide a full day (24 hours) into two periods: service operating hours (6:00–24:00) and off-duty hours (0:00–6:00). We assume that the fleet size is much larger than the number of operator-owned chargers. During service hours, vehicles' charging operations can only occur at operator-owned charging stations, but at the end of service hours, vehicles can go recharge at their own facilities or at other public charging stations for overnight charging. We assume that vehicles are fully charged at the beginning of the day. Time-of-use (ToU) energy prices are considered. Energy costs depend on the amount of charged energy and applied energy prices. When chargers are occupied, vehicles have to wait. No overlap is allowed for each charger, i.e. only one vehicle at a time. Charging facilities are assumed heterogeneous, and the number of chargers is fixed. Vehicles need to maintain a minimum reserve level. The objective of the operator is to maximize the total profit for the planning horizon (6:00-24:00) under stochastic customer demand.

We propose a sequential MILP approach that decomposes vehicle dispatching and charging operations into different planning horizons. First, a day-ahead charging schedule planning model devises vehicle-specific charging schedules to guide vehicles' charging times and target SoCs after recharging for each charging decision epoch (e.g. 30 minutes) for the day. This plan is adapted by a reactive model,

which adjusts the pool of go-charge vehicles based on current system state (current occupancy state of chargers, vehicles' states (location, SoCs, activities, etc.), and anticipated energy needs to the end of the day. An online vehicle-charger assignment model is applied to determine where to charge to minimize the total charging operational time per assignment epoch. For vehicle dispatching, a batch dispatching model is proposed to maximize the profit of vehicle-customer matching, given the customer's maximum waiting time and vehicles' SoC constraints. The decision time intervals for both vehicle dispatching and reactive model is based on a short-time horizon (e.g. 1 minute).

3.2. Vehicle dispatching

We adopt a batch dispatch optimization approach to match unserved requests with idled vehicles. Customer arrivals are stochastic and grouped into batches at the beginning of each decision epoch. A batch dispatching optimization is executed at the beginning of each batch decision epoch to maximize the profit of serving customers. Existing studies formulate this problem by neglecting the cumulative waiting time of customers in the unserved pool, resulting in customers leaving due to high waiting times (Ahadi et al., 2023). Different from the previous study, we integrate customer's maximum waiting time into the vehicle dispatching model to maximize the total profit of vehicles' dispatches. Let R_t denote the pool of unserved requests at the beginning of batch dispatch epoch t with the time interval $\Delta t = 1$ (minute), and V_t the set of idle vehicles at t . The batch dispatching problem is formulated as a MILP problem as follows.

P1: Batch dispatch

$$\max Z_1 = \sum_{r \in R_t} \sum_{v \in V_t} (g_r - \pi(\bar{d}_{o_r d_r} + \bar{d}_{v o_r})) m_{rv} \quad (1)$$

Subject to

$$\sum_{v \in V_t} m_{rv} \leq 1, \forall r \in R_t \quad (2)$$

$$\sum_{r \in R_t} m_{rv} \leq 1, \forall v \in V_t \quad (3)$$

$$E_v^{min} \leq e_{vt} - \mu(\bar{d}_{o_r d_r} + \bar{d}_{v o_r}) + M_1(1 - m_{rv}), \forall r \in R_t, v \in V_t \quad (4)$$

$$W_{rt} + \bar{t}_{v o_r} x_{rv} \leq W^{max} + M_2(1 - m_{rv}) \quad (5)$$

$$m_{rv} \in \{0,1\}, \forall r \in R_t, v \in V_t \quad (6)$$

The objective function (1) maximizes the profit of vehicle dispatch where the net profit of a customer-vehicle match (r, v) is calculated as the service fare g_r deduced by the vehicle's travel cost $\pi(\bar{d}_{o_r d_r} + \bar{d}_{v o_r})$; here o_r, d_r are the origin and destination of customer r , and $\bar{d}_{v o_r}$ is the distance from the vehicle's current location to pick up customer r . Constraints (2)-(3) ensure that one vehicle can serve at most one customer and vice versa. Constraint (4) ensures that a matched vehicle needs to have sufficient energy to reach the pickup location of the assigned customer and serve that trip. Constraint (5) ensures customers' waiting time cannot exceed a maximum threshold W^{max} (e.g., 7-10 minutes). Note that W_{rt} is customer r 's cumulative waiting time up to t . M_1 and M_2 are large positive numbers based on the bigM method to solve the mixed integer linear programming problem. Note that unassigned customers wait in the system to be assigned until the next decision epoch $t + 1$. If a customer's maximum waiting time is reached, they leave the system and are not served by the service. The service fare of a ride r is composed of a base rate β_0 and a distance-based operating fee, i.e., $g_r = \beta_0 + \beta_1 \bar{d}_{o_r d_r}$ with β_1 being the operating fee per kilometer traveled.

3.3. Day-ahead charging schedule planning and online vehicle-charger assignment

To better utilize limited operator-owned chargers, a day-ahead charging schedule plan model is proposed to minimize the overall charging operational costs by considering charging access costs, ToU energy costs, and opportunity costs for charging operations (including charging time and expected waiting time for charging). Let V denote the set of vehicles, H the planning horizon and S the set of chargers. H is divided into a set of charging decision epochs with a homogeneous interval (e.g. 30 minutes). The day-ahead charging planning model aims to determine when and target SoC for each epoch in H given vehicles' driving (energy) needs and charging infrastructure constraints for the day. As charging speed decreases significantly when the vehicle's SoC is above around 80% of its battery capacity (Froger et al., 2019), vehicles are not to charge above this threshold to save charging times during service hours. The problem is formulated as a MILP over a reduced and relevant subset $H^\ell = \{1, 2, \dots, n_{H^\ell} + 1\}$ where h starts from 1, denoting the first charging decision epoch with SoC lower than E_v^{max} (80% of battery capacity) based on the average energy consumption δ_h of vehicles. The end $n_{H^\ell} + 1$ corresponds to 24:00.

P2: Day-ahead charge schedule planning

$$\min Z_2 = \sum_{v \in V} \sum_{h \in H^\ell} \sum_{s \in S} \left((p_h + \frac{\gamma}{\varphi_s}) y_{hs}^v + (C + \gamma \bar{W}_{hs}) x_{hs}^v \right) \quad (7)$$

Subject to

$$\sum_{s \in S} x_{hs}^v \leq 1, \forall v \in V, h \in H^\ell \quad (8)$$

$$\sum_{v \in V} x_{hs}^v \leq 1, \forall s \in S, h \in H^\ell \quad (9)$$

$$e_{v,h+1} \leq e_{vh} - \delta_h \left(1 - \sum_{s \in S} x_{hs}^v \right) + \sum_{s \in S} y_{hs}^v, \forall v \in V, h \in H^\ell \quad (10)$$

$$e_{v,h+1} \geq e_{vh} - \delta_h \left(1 - \sum_{s \in S} x_{hs}^v \right) + \sum_{s \in S} y_{hs}^v, \forall v \in V, h \in H^\ell \quad (11)$$

$$\alpha_s \leq \left(\frac{y_{hs}^v}{\varphi_s} \right) + M_3 (1 - x_{hs}^v), \forall v \in V, h \in H^\ell, s \in S \quad (12)$$

$$E_v^{min} \leq e_{vh} \leq E_v^{max}, \forall v \in V, h \in H^\ell \cup \{n_{H^\ell} + 1\} \quad (13)$$

$$e_{v1} = E_0, \forall v \in V \quad (14)$$

$$y_{hs}^v \leq M_4 x_{hs}^v, \forall v \in V, h \in H^\ell, s \in S \quad (15)$$

$$0 \leq y_{hs}^v \leq Y_s^{max}, \forall v \in V, h \in H^\ell, s \in S \quad (16)$$

$$x_{hs}^v \in \{0, 1\}, \forall v \in V, h \in H^\ell, s \in S \quad (17)$$

The objective function (7) minimizes total charging costs for the planning horizon H^ℓ . The first term in Eq. (7) is related to charging costs for y_{hs}^v where p_h denotes the average energy price on h . φ_s is the charging power of charger s . γ is the average profit per vehicle-minute traveled based on the realized customer service/profit on the previous days. The second term is related to charging access distance costs C and expected waiting times \bar{W}_{hs} when arriving at the charger s at the beginning of epoch h . Eqs. (8) and (9) state that each vehicle can be assigned to at most one charger, and each charger can be assigned to at most one vehicle for each h , respectively. Eqs. (10) and (11) state vehicles' SoC changes from h to $h + 1$ with the charged amount of energy when recharging and with average energy consumption δ_h of vehicles otherwise. Eq. (12) states that a minimum charging time α_s (e.g. 10 minutes) is implied for each charging operation. Eq. (13) and (14) set the range of e_{vh} and the initial battery level E_0 at the beginning of $h = 1$, respectively. Eq. (15) binds x_{hs}^v and y_{hs}^v . Eq. (16) ensures the maximum amount of energy can be recharged from charger s during one charging decision epoch. M_3 and M_4 are big positive numbers with $M_3 = \Delta h$ and $M_4 = \max_{s \in S} \{Y_s^{max}\}$. The model parameters δ_h , \bar{W}_{hs} , γ , and C can be estimated based on historical vehicle driving and charging data.

Based on the outputs of P2 (i.e., the solution of e_{vh} , x_{hs}^v and y_{hs}^v), the operator obtains a schedule to assign vehicles to charge and their target SoCs after recharge over H . This schedule is then adapted based on a reactive model to determine the amount of energy to be charged and where to charge for vehicles. This reactive model maintains a pool of go-charge-vehicles based on the charging plan (excluding vehicles currently serving customers), which is adapted with additional vehicles to recharge; either with low SoC (i.e. less than 20% of their battery level) or previously delayed vehicles for charging or due to the number of go-charge-vehicles exceeds the number of chargers. An online vehicle-to-charger assignment model below is applied to minimize total charging operational times for vehicle-to-charger assignment. A more detailed description is presented in the simulation framework (Algorithm 1). The online vehicle-to-charger assignment problem is formulated as a MILP as follows.

P3: Online vehicle-charger assignment

Let V_t be the set (pool) of to-recharge vehicles at the current decision epoch t (same as the batch assignment, corresponding to t minutes from the beginning of the service). Given the current location of vehicles and the utilization state of chargers, the objective function (18) aims to minimize the total charging access time (\bar{t}_{vs}) and waiting time (\bar{W}_{vs}), and charging time (ψ_{vs}/φ_s) of the assignment of vehicles to chargers. Given the current utilization state of chargers, \bar{W}_{vs} is the waiting time that vehicle v would experience if it departs immediately to go to charger s . The operator looks across all current charger queues and obtains the waiting time at every charger. This information can be obtained online from the operator's charging network management system.

$$\min Z_3 = \sum_{v \in V_t} \sum_{s \in S} ((\bar{t}_{vs} + \bar{W}_{vs})x_{vs} + \psi_{vs}/\varphi_s) \quad (18)$$

Subject to

$$\sum_{s \in S} x_{vs} = 1, \forall v \in V_t \quad (19)$$

$$\sum_{v \in V_t} x_{vs} \leq 1, \forall s \in S \quad (20)$$

$$0 \leq e_v - \mu \bar{d}_{vs} x_{vs} + M_2(1 - x_{vs}), \forall v \in V_t, s \in S \quad (21)$$

$$\bar{E}_v \leq e_v - \mu \bar{d}_{vs} x_{vs} + \psi_{vs} + M_2(1 - x_{vs}), \forall v \in V_t, s \in S \quad (22)$$

$$\alpha_s \leq \left(\frac{\psi_{vs}}{\varphi_s}\right) + M_1(1 - x_{vs}), \forall v \in V_t, s \in S \quad (23)$$

$$\psi_{vs} \leq M_1 x_{vs}, \forall v \in V_t, s \in S \quad (24)$$

$$0 \leq \psi_{vs} \leq Y_s^{max}, \forall v \in V_t, s \in S \quad (25)$$

$$x_{vs} \in \{0,1\}, \forall v \in V_t, s \in S \quad (26)$$

Constraints (19) and (20) ensure that each vehicle is assigned to exactly one charger, and each charger can be connected to at most one vehicle when the number of to-recharge vehicles is no less than that of chargers. In the other case, these two equations are replaced by Eqs. (26)-(27).

$$\sum_{s \in S} x_{vs} \leq 1, \forall v \in V_t \quad (27)$$

$$\sum_{v \in V_t} x_{vs} = 1, \forall s \in S \quad (28)$$

Eq. (21) ensures that the vehicle's SoC is always non-negative when arriving at the charger's location. Eq. (22) states that vehicle v needs to be recharged to the target SoC \bar{E}_v based on the day-ahead charging plan. Note that if a vehicle is delayed to be added to the pool due to serving customers, its target SoC remains the planned one based on the output of P2. As aforementioned, when the additional go-charge vehicles' SoCs are below a threshold θ (i.e. 20% of their battery capacity), they are added to the pool. These vehicles' respective target SoCs are set based on the average energy consumption δ_h (estimated

from historical data) by anticipating their energy consumption to the end of the day. To maximize vehicles' availability, vehicles' SoC at the end of the day should be as close as possible to E_v^{min} . For this purpose, we apply the following rule to determine vehicles' target SoCs when their SoCs are below θ . Let SoC_v^t denote vehicle v 's SoC¹ at t , and $h(t)$ be the corresponding h index of t . The target SoC of vehicle v when adding it to the to-charge vehicle pool at t is defined as

$$SoC_v^{target}(t) = \min(\tilde{E}_v, SoC_v(t) + \vec{E}_v(t)) \quad (29)$$

where $\vec{E}_v(t)$ is the energy needed to the end of the day, calculated as $\vec{E}_v(t) = \sum_{h=h(t)}^{n_H} \delta_h - m\delta_h$ with m being the approximated number of epochs whose total energy consumption is around E_v^{min} (i.e. $m\delta_h \leq E_v^{min}$). In doing so, Vehicles' SoCs at the end of the day would be a little more above E_v^{min} , given vehicles' current SoC is around θ . To further reduce vehicles' waiting time for charging, we can set \tilde{E}_v as $rand(0.5B, E_v^{max})$ where B denotes the vehicle's battery capacity. This policy is more flexible than using E_v^{max} as vehicles can recharge again sometime later as far as their SoCs are below θ . Eq. (23) ensures a minimum charging time α_s when vehicles go charging. Eq. (24) binds the variables x and y . Eq. (25) specifies the maximum energy that can be charged for one charging decision epoch. Note that if no feasible solutions can be found, vehicles with the highest SoCs are removed from V_t , and then the problem is solved again until the optimal solution is found. The removed vehicles remain idled and can be dispatched to serve customers. If the removed vehicles are not dispatched for serving customers (remain idled) during t , they are added to the pool for charging at $t + 1$. Note that for each vehicle-to-charger assignment epoch t , V_t is filtered by retaining a subset of vehicles in V_t where the calculated amount of energy to be charged (depending on vehicles' current SoC and their target \tilde{E}_v) needs to be at least equivalent to the amount of charging α minutes (minimum charging duration) on a fast charger. If the amount of energy to be charged is below this minimum amount of energy, vehicles remain idled for serving customers. In doing so, multiple short-duration recharging operations with short charging times can be avoided, significantly reducing the operator's total charging access costs.

Algorithm 1 presents the pseudocode of the simulation framework. The simulation technique is based on the discrete event simulation technique but integrates vehicle dispatching and charging decisions for each short planning horizon (1 minute). Step 1 reads the input data. Step 2 estimates the parameters used for the day-ahead charging planning model (described in more detail in Sect. 4). Step 3 solves P2 to obtain the day-ahead charging plan of vehicles. Step 4 sets up the initial condition for the simulation. Step 5 is the loop of the simulator clock for batch dispatching where t corresponds to minutes after the start (6:00), and T corresponds to the end of the day (24:00). Note that we use a continuous time to track the system state in the simulator. Steps 6 to 8 add vehicles to the pool based on the day-ahead charging plan. Step 9 adds additional vehicles to the pool if their SoCs are below the threshold θ . Steps 10-13 filter idled vehicles in the pool and assign them to chargers for recharge by solving P3. Steps 14-16 update the list of idled vehicles and unserved customers and dispatch vehicles to serve customers based on P1. Then update the system state until the end of t . Note that time is continuous in our simulation implementation and the system state is updated accordingly with the occurring times of different events.

Algorithm 1. Simulation framework for dynamic charging planning, vehicle-to-charger assignment, and batch dispatch.

-
1. Input: Time-dependent energy prices, customer demand, a fleet of vehicles, and charging facilities.
 2. Compute the average energy consumption (δ_h) and average charging waiting times ($\bar{W}_{h,s}$) of vehicles at chargers per charging decision epoch up to the previous day.
 3. Solve the day-ahead charging planning problem P2 to get initial charging plans of vehicles for the planning horizon (i.e. 6:00-24:00).
 4. Initialization: Initialize SoCs and locations of vehicles. Set up the pool of go-charge vehicles Ω as empty.
 5. **for** $t = 1, 2, \dots, T$
 6. **if** $t \% \Delta h = 0$
 7. Add the subset of idled vehicles planned to be recharged at the beginning of h to Ω
-

¹ SoC is the percentage of vehicles' battery capacity, i.e. $0 \leq SoC \leq 1$.

-
8. **End**
 9. Find the subset of idled vehicles with SoCs lower than θ and add them to Ω .
 10. Find the subset of vehicles $\tilde{\Omega}$ in Ω that are idled and have to charge to their target SoCs satisfying a minimum amount of charged energy requirement.
 11. **If** $\tilde{\Omega}$ is not empty
 12. Solve P3 for $\tilde{\Omega}$ and assign vehicles to their assigned chargers. If there are no solutions, relocate the vehicle with the highest SoC from $\tilde{\Omega}$ to Ω and solve P3. Continue until a feasible solution is found.
 13. **end**
 14. Update the lists of unserved customers. Remove vehicles going for charging from the list of idled vehicles.
 15. Solve the batch dispatching problem P1 and dispatch vehicles to serve customers.
 16. Update the system state to the end of t .
 17. **end**
-

3.4. Benchmark charging policies

To validate the proposed methodology, four benchmark charging policies selected from the literature are compared. These policies assume that vehicles go to recharge when their SoCs are lower than a pre-defined threshold. Different from existing studies that assume vehicles are willing to wait without limits at a charger (Jamshidi et al., 2021), we consider more realistic queuing scenarios at chargers for the benchmark policies by assuming a maximum waiting time limit in a queue (i.e. 15 minutes, identical for all vehicles). Vehicles are assigned to chargers based on the used charging policy. When arriving at the assigned charging stations, if the waiting time exceeds the maximum threshold, vehicles move away to another charger with the least waiting time when their SoCs are feasible to reach there. In case the vehicle's SoC is too low to reach the targeted charger, vehicles go to the nearest one (if the vehicle's SoC is feasible) or remain at the same charger (if the vehicle's SoC is not feasible). This allows not to have unrealistically too long queue at charging stations. The benchmark charging policies are described as follows.

- a. Nearest charging policy (Nearest)(Bischoff and Maciejewski, 2014): Vehicles go to the nearest charger to recharge to E_v^{max} (i.e. 80% of their battery capacity) when their SoCs are below the threshold θ (i.e. 20% of their battery capacity).
- b. Fastest charging policy (Fastest): Vehicles go to the fastest charger to recharge to E_v^{max} when their SoCs are below the threshold θ . In case there is more than one fastest charger, a randomly selected one is used. Note that if charging demand on fast chargers is not high (no congestion), one can assign vehicles to the nearest one. On the contrary, when the number of fast chargers is scarce, using this random-assignment policy allows not to assign too many vehicles to a geographically well-situated charging station (e.g. the one located at the middle of our study area), resulting in over-saturated utilization of certain fast chargers/charging stations.
- c. Charging operational time minimization approach (MinChgOpt)(Ma and Xie, 2021): When vehicles' SoCs are below the threshold, vehicles are assigned to the charger with minimum charging operational time to charge to E_v^{max} , including access time, waiting time when arriving at chargers and charging time.
- d. Dynamic charging threshold policy (DynaThreshold)(Ahadi et al., 2023): Different from the above benchmark policies, DynaThreshold activates vehicles' charging operations earlier when their SoCs are still much higher than the threshold in order to avoid charging during peak charging demand periods in the afternoon. In doing so, vehicles can save (charging) waiting time and the charging facility can be utilized more effectively. We adopt the hourly dynamic charging thresholds used in Ahadi et al. (2023), where the average hourly charging threshold in the morning is around 50% while it becomes around 30% in the afternoon (see Table 1). When going charging, vehicles are charged to E_v^{max} so we expect that vehicles charges fewer amount of energy compared to the situation in the afternoon.

Table 1. Dynamic hourly SoC threshold for activating charging operations (Ahadi et al., 2023).

Hour (morning)	1	2	3	4	5	6	7	8	9	10	11	12
SoC threshold*	0.45	0.6	0.65	0.62	0.58	0.55	0.52	0.5	0.4	0.4	0.4	0.4
Hour (afternoon)	13	14	15	16	17	18	19	20	21	22	23	24
SoC threshold	0.38	0.35	0.32	0.25	0.25	0.2	0.2	0.25	0.27	0.35	0.35	0.4

*: % of vehicles' battery capacity.

4. Computational study

In this section, we first describe the test instance and parameter setting based on Manhattan yellow taxi data. Then we present the computational results for different demand scenarios. A sensitivity analysis is conducted to evaluate the impact of different model parameters.

4.1. Test instance generation

We test the proposed dynamic charging planning approach on a Manhattan-like 4x20 km² area. We assume that the fleet size is 100 homogeneous EVs. Demand data is randomly drawn from the trips of New York yellow taxi data² on a typical weekday in July 2019. The service operating hours are 6:00 – 24:00. Two demand scenarios are considered: low demand with 3000 customers/day and high demand with 4000 customers/day. As a comparison, the average daily trips per yellow taxi in July 2019 was 20.5 trips, according to the Taxi and Ride-hailing Usage in New York City dashboard³. As the customer's origins and destinations are unavailable, we generate them randomly in the study area with an assumed minimum trip length of 5 km which might be somewhat higher than real trip distance in Manhattan. We assume that the origins of customers' requests are within the 4x20 km² area, while their destinations could be outside this area. We randomly generate 15 independent customer demand datasets for each scenario, of which 10 are used for the parameter estimation of P2 (i.e. δ_h , \bar{W}_{hs} and γ) and 5 are used to validate the proposed methodology). For the operator-owned charging infrastructure, we assume there are 6 fast and 6 slow chargers located at 4 different charging stations (i.e. each fast (slow) charging station has three fast (slow) chargers, see Figure 1). We locate one fast charging station around the bottom center and another around the center right based on the current public charging station locations in Manhattan⁴. The charging power is assumed 50 kWh (fast) and 11kWh (slow), respectively. For the fleet, we assume that vehicles are fully recharged during the night (the overnight charging cost is not the operator's concern) at their initial locations (assume they are randomly located in the study area). Figure 1 illustrates the charging station locations and initial locations of vehicles in the study area. The number of customer arrivals per 10 minutes for low and high-demand scenarios is shown in Figure 2. We can observe that both demand profiles are very irregular with higher peaks during certain time slots (e.g. 8:00-10:00, 12:00-13:00, and 15:00-18:00). The peak demand is around 60 customer arrivals per 10 minutes. We assume that Nissan Leaf e+ is the used vehicle with a battery capacity of 62 kWh and an energy consumption rate of 0.25 kWh/kilometer traveled (see Table 2). The impact of battery capacity on the performance of the proposed methodology will be analyzed in the sensitivity analysis. For energy prices, we assume that ToU energy prices change every 15 minutes based on the time-varying day-ahead electricity prices, adapted to the real charging fee of NYC public charging stations. For simplification, we assume that charging costs do not depend on the used type of chargers. In practice, there might have supplementary fee for using fast chargers. Figure 3 shows the ToU electricity prices per kWh charged over 4 consecutive days. The highest and lowest electricity prices are around 0.58 USD/kWh and 0.09 USD/kWh. Note that other practical ToU energy prices can be applied in practice. The detailed parameter setting for the computational study is shown in Table 2.

² <https://www.nyc.gov/site/tlc/about/tlc-trip-record-data.page>

³ <https://toddwshneider.com/dashboards/nyc-taxi-ridehailing-uber-lyft-data/>

⁴ <https://www.nyc.gov/html/dot/html/motorist/electric-vehicles.shtml#/find/nearest?location=NYC>

Table 2. Simulation parameter settings of the case study.

System parameter	Value
Fleet size	100
Number of charging stations	4
Number of chargers ¹	6 DC fast (50kW) and 6 slow chargers (11 kW)
Number of customers per day	3000 and 4000
Vehicle speed	30 km/hour
Taxi fare ²	$\beta_0 = \$8$ (base rate), $\beta_1 = 3.1$ (dollar/km) (operating fee)
Maximum waiting time of customers	10 minutes
Minimum charging duration (α_s)	10 minutes
Battery capacity ³ (B_v)	62 (kWh)
Travel distance cost ⁴ (π)	0.53 (dollars/km)
Energy consumption rate ³ (φ)	0.25 (kWh/km)
$E_{max}(E_{min})$	80% (10%) of B_v
E_{init}	62 (kWh)
Time-dependent energy price ⁵	Day-ahead electricity Prices (15-minute resolution)
Service time	6:00-24:00
Charging planning horizon	6:00-24:00
Charge decision time interval (Δh)	30 minutes
Batch dispatching time interval (Δt)	1 minute

Remark: 1. Based on the two main charger types used in New York City (Taxi & Limousine Commission, 2022). 2. Approximated based on the current yellow taxi fare in NYC. The base fee includes the surcharges (<https://www.nyc.gov/site/tlc/passengers/taxi-fare.page>). 3. Adapted from the characteristics of Nissan Leaf e+ (<https://evadepot.com/calc/tesla-supercharger-charging-cost-calculator>). 4. Based on Ahadi et al. (2023). 5. Adapted from <https://transparency.entsoe.eu/>, bidding zones GE_LU, July 2019. The adapted electricity price variation range covers the real charge fee in New York City (\$0.39 per kWh consumed; see <https://www.nyc.gov/html/dot/html/motorist/electric-vehicles.shtml#/dc>).

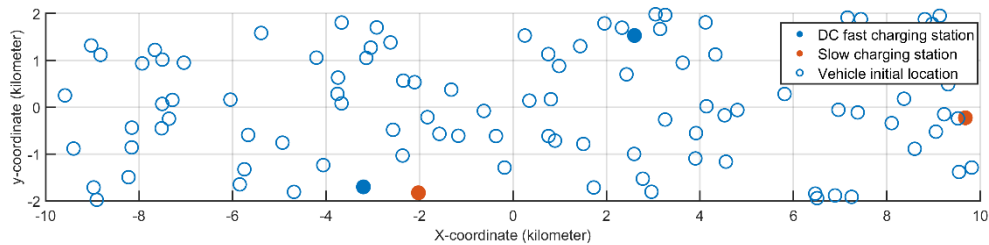


Figure 1. Charging station distribution in the study area. There are 4 charging stations, each with three chargers of the same type. A total of 6 DC fast chargers (50kW) and 6 slow chargers (11kW).

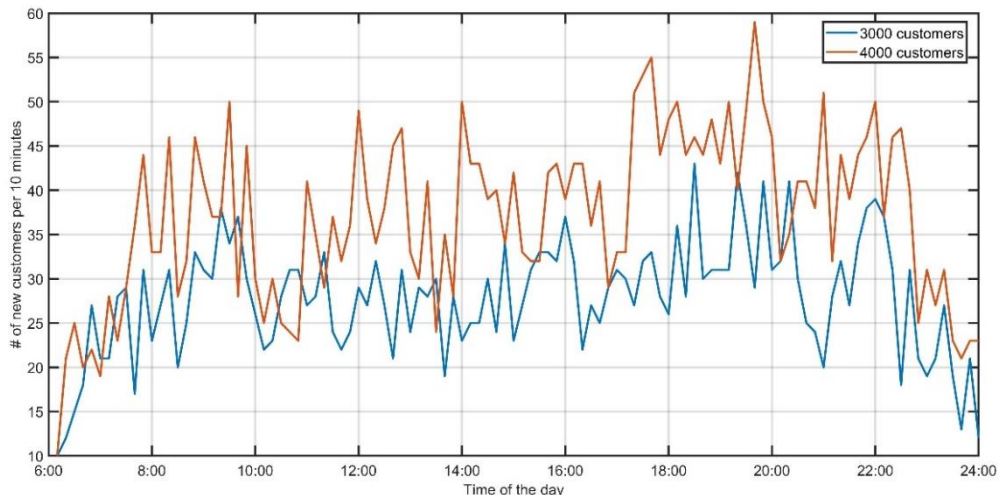


Figure 2. An example of customer arrival intensity per 10 minutes for two different demand scenarios.

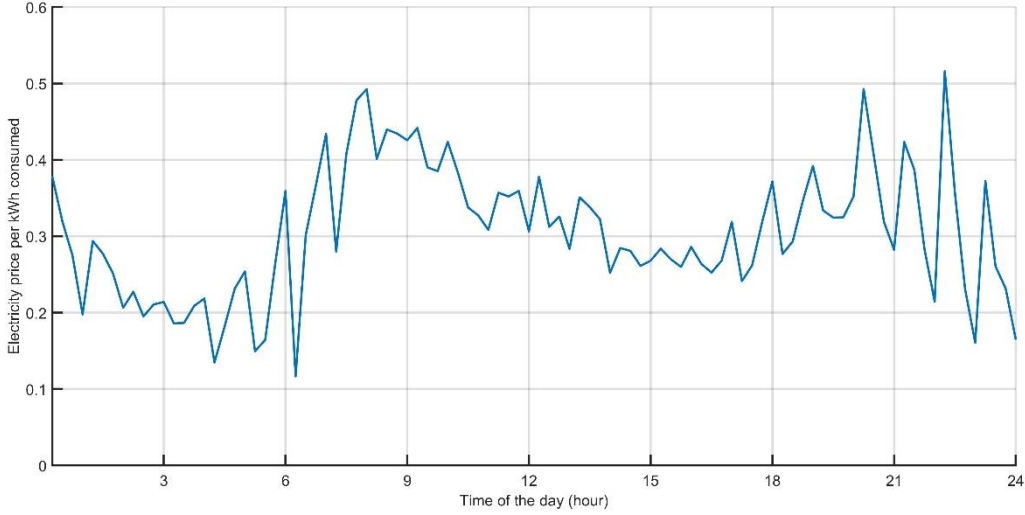


Figure 3. Electricity prices per kWh charged for 24 hours.

4.2. Results

We test the performance of the CongestionAware charging policy on the test instances and compare it with the benchmark approaches. The implementation is based on Julia on a laptop with Intel(R) Core(TM) i7-11800H and 64 GB memory. The MILP models P1 to P3 are solved using Gurobi. We define a set of key performance indicators (KPIs) to evaluate the performance of different charging policies, including total profit (PF), revenue (TR), travel costs (TTC), charging costs (CC), energy charged (ENG), customer service rate (SR), vehicle kilometer traveled (KMT), charging waiting time (TW), and charging time (TC). The acronyms and used measurement units are shown in Table 3.

Table 3. Acronyms used in the tables of the computational studies.

Acronym	Meaning	Unit
PF	Profit	1000 USD
TR	Revenue	1000 USD
TTC	Travel costs	1000 USD
CC	Charging costs	1000 USD
ENG	Amount of charged energy	kWh
SR	Service rate	%
KMT	Vehicle-kilometer traveled	1000 kilometers
TW	Charging waiting time	hour
TC	Charging time	hour

a. Model parameter estimation and base results

The model parameters for the day-ahead charging planning P2 are C , δ_h , γ , and \bar{W}_{hs} , which need to be estimated based on historical driving and charging operations data. We estimate the average charging access cost C as approximately \$2.7 based on an approximate average distance costs to the charging stations. δ_h is estimated by conducting a simulation using internal combustion engine vehicles. For \bar{W}_{hs} and γ , we simulate the system for the two demand scenarios using the Fastest charging policy and obtain their respective averaged values. As mentioned previously, 10 independent datasets are used for the simulation to obtain these parameters for each demand scenario. Then we test the performance of the proposed method on the 5 test instances (days) and report the average results.

The results for two demand scenarios with 3000 and 4000 customers a day are shown in Table 4. Compared with the benchmark, the CongestionAware policy has the highest profit for both scenarios.

Total profit increases 7.65%-10.69% for the c3000 scenario and 8.76%-15.05% for the c4000 scenario. Regarding service rate, the CongestionAware policy outperforms the benchmark by increasing 7%-10.8% and 7.9%-12.3% for the c3000 and c4000 scenarios, respectively. For the c3000 scenario, the benchmark charging policies result in much higher total charging waiting times (doubled or tripled) than the CongestionAware policy. The total charged time is almost doubled, and the total charged energy is higher than the CongestionAware policy. As a result, the service rates of the benchmark policies are much lower (from -7.37% to -11.12%) compared with the CongestionAware policy. For the c4000 high-demand scenario, similar results can be observed. The CongestionAware policy has a much lower charging waiting time and charging time than the benchmark policies, resulting in a higher service rate (76.5%) and profit (\$88.08k). As the service rate is higher for the CongestionAware policy, which means (inevitably) more KMT to serve more customers with more energy use and higher TTC. The energy use per served customer is 2.6411 (2.7675) kWh for the c3000 (c4000) scenario for the CongestionAware policy, which is lower (around -3.2% for the two scenarios) than the benchmark policies (2.7149 to 2.7269 kWh (c3000 scenario) and 2.8543 to 2.8578 kWh (c4000 scenario)). Note that among the benchmark policies, the DynaThreshold has the best performance because vehicles go to recharge their vehicles earlier and avoid charging congestions in the peak charging demand period (to be explained below).

Table 4. Comparison of the KPIs for different charging policies.

Scenario	Charging policy	PF	TR	TTC	CC	ENG	SR	KMT	TW	TC
c3000 (3000 requests)	Nearest	73.02	88.93	14.72	0.89	2824	84.9%	27.8	111.7	94.1
	Fastest	73.46	89.52	14.83	0.92	2935	85.7%	28.0	94.0	94.1
	MinChgOpT	74.45	90.67	15.02	0.94	3011	86.9%	28.3	77.1	92.6
	DynaThreshold	75.08	92.06	15.31	1.06	3430	88.7%	28.9	97.2	107.8
	CongestionAware	80.59	97.93	16.07	0.80	2556	95.7%	30.3	36.0	52.4
c4000 (4000 requests)	Nearest	76.55	93.12	15.54	0.82	2657	64.2%	29.3	136.1	93.1
	Fastest	77.31	94.07	15.69	0.84	2745	64.8%	29.6	100.4	93.0
	MinChgOpT	77.56	94.37	15.75	0.85	2796	65.1%	29.7	99.2	93.0
	DynaThreshold	80.98	99.41	16.62	1.15	3751	68.6%	31.4	135.7	120.3
	CongestionAware	88.08	107.64	17.95	1.04	3280	76.5%	33.9	48.4	68.5

Figures 4 and 5 analyze the number of vehicles charging (subfigures (b)) and of waiting (subfigures (c)) for the day and residual battery levels of vehicles (subfigures (d)) at the end of the day for different charging policies. Subfigure (a) shows the average waiting time at fast chargers that vehicles would have experienced using the Fastest charging policy. For the c3000 scenario, Subfigure (a) in Figure 4 shows the charging waiting times at fast chargers increase significantly from the 10th hour from the beginning of service (16:00) to the 14th hour (20:00) when using the Fast charging policy. As a result, the day-ahead charging plan model devises a charging plan to avoid vehicle charging and waiting during peak charging demand hours. Subfigure (b) shows the CongestionAware charging policy activates vehicle charging operations earlier to reduce charging congestion compared to the benchmark. During peak charging demand hours (from 10th to 16th hours), the number of vehicles charging is around 14 per 30 minutes, lower than the benchmark with around 1 or 2 more vehicles. As this policy anticipates vehicles' energy (driving) need to the end of the day, fewer energy are charged in the late evening, resulting in a higher service rate and fewer vehicles charging and waiting. Subfigure (c) shows that using the first three benchmark policies results in high charging congestion (more vehicles waiting for charging) during the evening peak (from the 10th hour to the 14th hour) due to the increasing number of vehicles' SoCs falling below the threshold of 20% battery capacity. The charging demand decreases after the 14th hour and then increases again in the late evening. For the DynaThreshold policy, the number of vehicles waiting increases gradually from the 6th hour until the end of the day. This is because the hourly charging thresholds for the second half of the day are lower (around 50% in the morning and 30% in the afternoon on average), resulting in more vehicles charging and waiting at the chargers due to charging longer time in the afternoon and evening, and insufficient number of fast chargers in the system. However, this DynaThreshold policy performs better than the other three benchmark policies as it applies a smarter

partial recharge policy. Subfigure (d) shows the distributions of vehicles' SoCs at the end of the day. We can observe that the medians of vehicles' SoC using the benchmark policies are around 14kWh (Nearest, Fastest, and MinChgOpT) and 19kWh (DynaThreshold), respectively, whereas 7.2kWh for the CongestionAware policy. For the c4000 scenario, the charging congestion starts earlier (mainly located between the 8th and 12th hours instead of between the 10th and 14th hours; see subfigures (a) of Figures 5 and 4) due to higher customer arrival intensity for the c4000 scenario. Consequently, the obtained day-ahead charging plan reacts in response to the charging waiting time signals, resulting in significantly higher charging operations in the early hours of the day. As the CongestionAware policy applies a smarter partial recharge strategy (Eq. (29)) to delay vehicles' charging operations when charging waiting time on a queuing charger exceeds a maximum threshold (e.g. 30 minutes) and minimize the charging operational times for online vehicle-to-charger assignment, it allows significantly increasing vehicles' availability to serve customers. Interestingly, the distribution of vehicles' SoCs at the end of the day has similar medians for all the charging policies (around 7.3 kWh), but the benchmark policies have a much higher 75-percentile (around 20kWh or more) compared with the CongestionAware policy (7.4kWh).

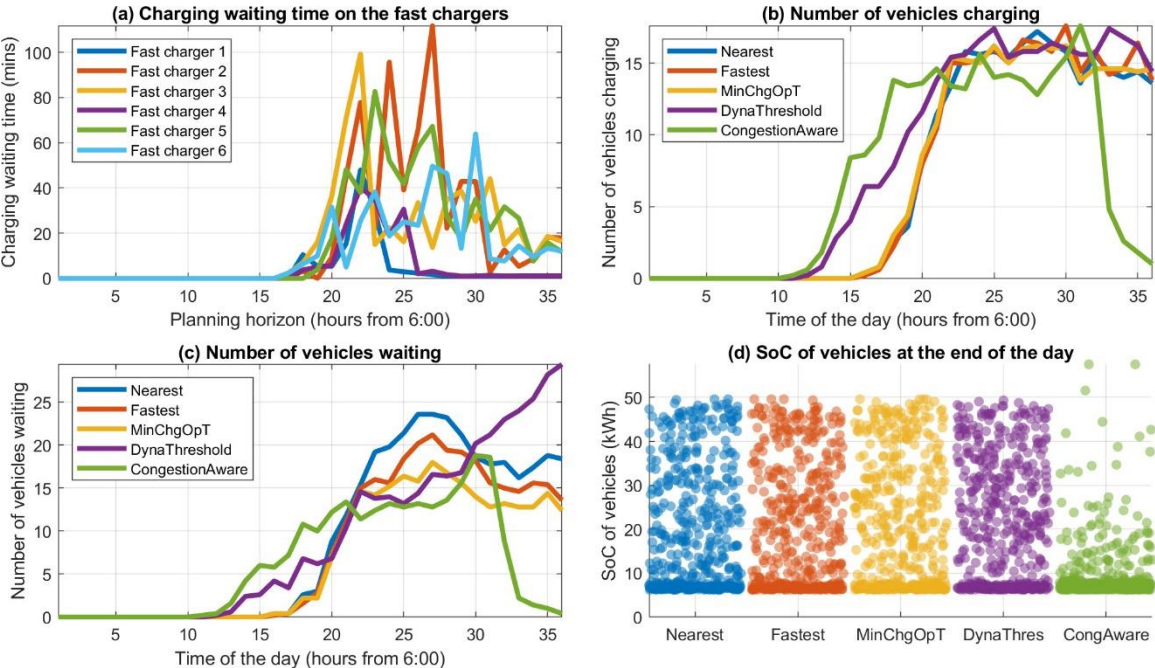


Figure 4. Comparison of number of vehicles charging, vehicles waiting, and SoCs of vehicles at the end of the day (c3000 scenario).

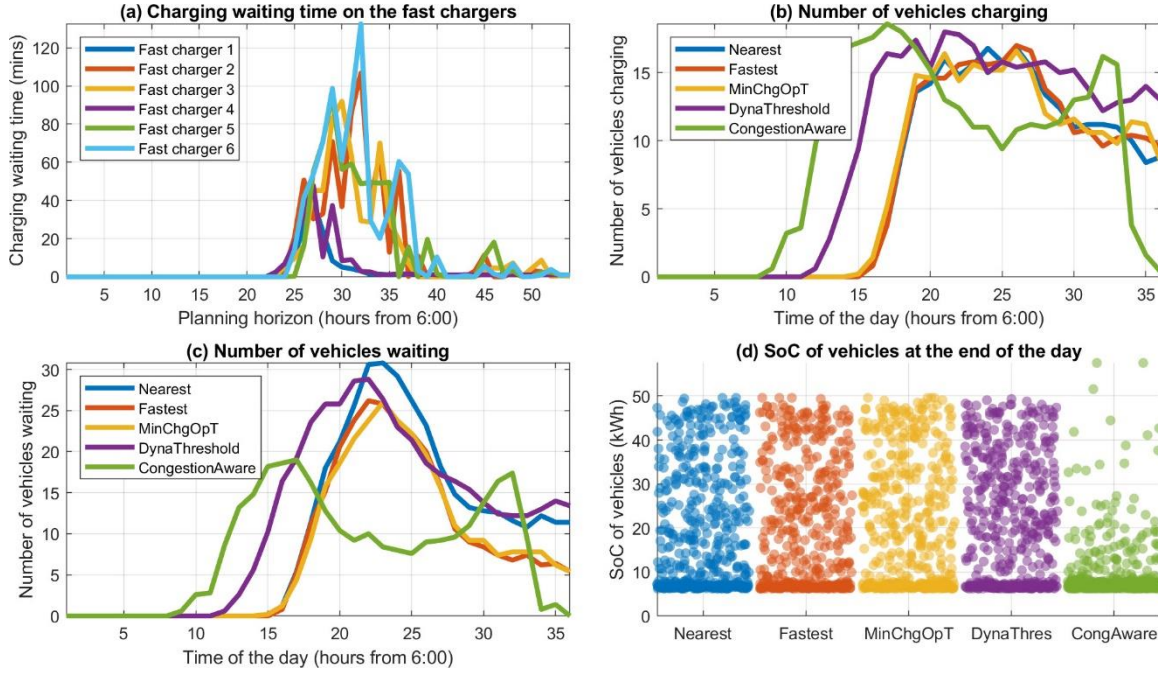


Figure 5. Comparison of number of vehicles charging, vehicles waiting, and SoCs of vehicles at the end of the day (c4000 scenario).

b. Analysis of realized charging sessions and occupancy state of chargers

Figure 6 compares the distributions of charging session durations using different charging policies where Subfigure (a) is related to the c3000 scenario while Subfigure (b) to c4000 scenario. The CongestionAware policy has a significantly lower charging duration per charging session compared with the benchmark. For the c3000 scenario, the median charging session duration and amount of charged energy for the CongestionAware policy is 19.3 minutes (S.D. = 9.2 minutes) and 15.4 kWh (6.6 kWh), respectively. For the c4000 scenario, the median duration of charging sessions and charged amount of energy is 23.7 minutes (S.D. = 13.5 minutes) and 18.2 kWh (S.D. = 9.3 kWh), respectively. Compared with the CongestionAware policy, the median charging durations of the benchmark policies are much higher (around 50 minutes for both scenarios).

Figure 7 shows the number of vehicles on fast and slow chargers over different charging policies where Subfigures (a) (fast chargers) and (b) (slow chargers) are related to using the benchmark policies, while Subfigures (c) (fast chargers) and (d) (slow chargers) to using the CongestionAware policy. For the CongestionAware policy, all fast chargers (6 in total) are almost fully occupied from the 10th to 16th hours. The CongestionAware policy has a higher occupancy rate on fast chargers compared to the benchmark between the 5th to 10th hours. For slow chargers, using the benchmark policies results in a higher utilization rate of slow chargers (11kW) in the evening. This is because vehicles move away from fast chargers after waiting for a maximum waiting time (15 minutes) and go to another fast/slow charger with the least waiting times. Note that we might apply different waiting policies at chargers. We test the effect of applying different waiting policies (i.e. no limit waiting, charger-chasing using fast chargers only or charger-chasing using fast or slow chargers). The results show the above charger-chasing policy has better performance compared to the other two waiting policies (see Appendix A). The utilization rate on slow chargers is very low (0 most of the time or <1 between the 10th and 16th hours) when using the CongestionAware policy. This is because the online vehicle-to-charge assignment model P3 minimizes the total charging operation times (including charging access time, waiting time, and charging time) under the constraints that the SoCs of vehicles after recharge need to be no less than their target energy levels (Eq. (22)) and satisfy a minimum charged amount energy requirement. Given the fact that the charging power of slow chargers is 11kWh, the maximum amount of energy can be charged on a slow charger during one charging decision epoch (30 minutes) is quite limited (5.5kWh). If the difference between vehicles' target energy levels and their SoCs is higher than this amount, vehicles will not be assigned to

slow chargers. Consequently, slow chargers' utilization rate is much lower than that of fast chargers, for which vehicles can get charged 25kWh for a 30-minute charging time.

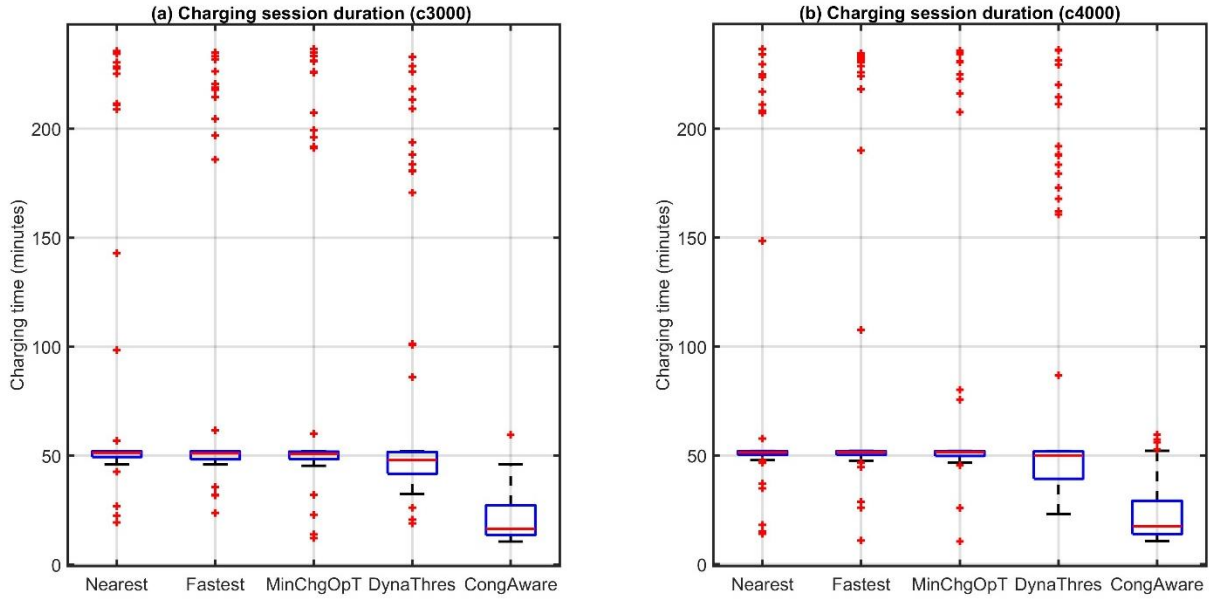


Figure 6. Distribution of the charging session durations for the c3000 scenario (on the left) and the c4000 scenario (on the right).

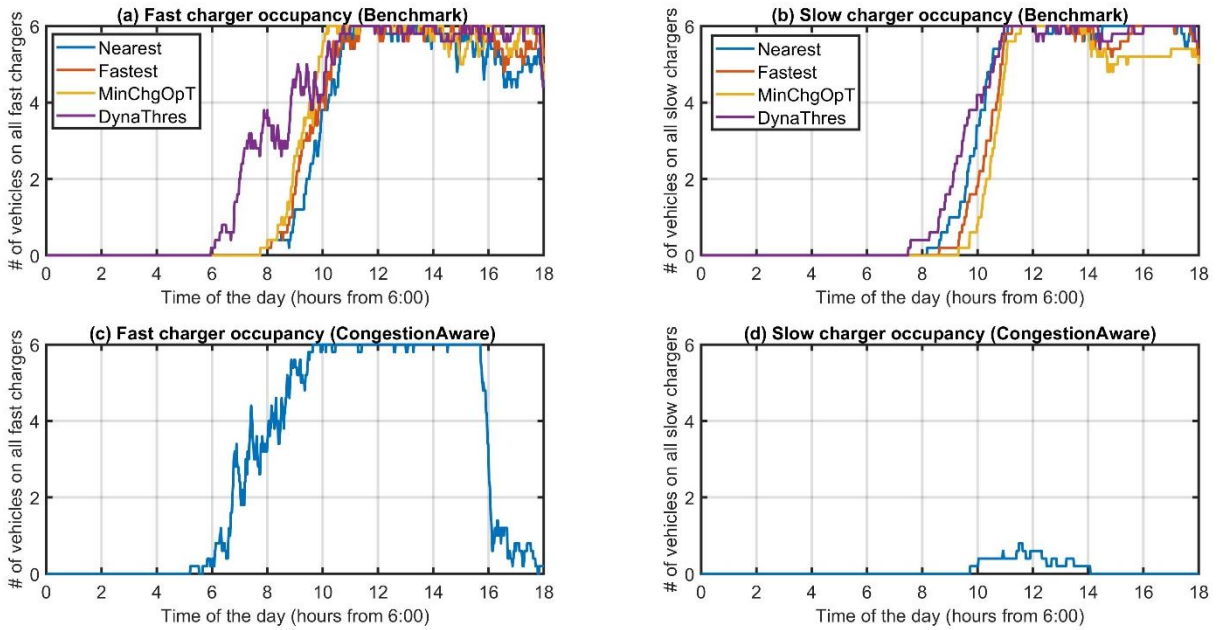


Figure 7. Comparison of the average number of vehicles on fast chargers (on the left) and slow chargers (on the right) using different charging policies for the c3000 scenario.

c. Effects of vehicles' energy need anticipation and time-of-use energy prices

For the CongestionAware policy, we further investigate the benefits of the energy-need anticipation strategy to determine the target energy level (Eq. (29)) by comparing an alternative without using it, i.e. vehicles charge to E_v^{max} (80%) from their current battery levels. The results are shown in Table 5. We can observe that using this strategy allows for reducing vehicles' charging waiting time (-14.7% to -18.4%) and increasing customers' service rate (+1.5 to +3.9%) and profits (+1.6% to +4.8%). When not applying this anticipative strategy, the CongestionAware policy still significantly outperforms the benchmark in terms of total profit and service rate (see Table 4). In terms of the benefits of applying ToU energy prices, Table

6 compares the KPIs with and without using ToU energy prices (i.e. using a constant energy price of 0.33 USD/kWh to get the day-ahead charging plan but applying ToU policy for the test instances). The results show a small amount of cost savings could be obtained (CC column for the c3000 scenario) as the day-ahead charging planning model P2 minimizes the total charging costs over the planning horizon. However, its effect is less significant than using energy-need anticipation for the reactive model.

Table 5. Comparison of the CongestionAware policy with and without anticipating energy needs.

Scenario	Anticipate	PF	TR	TTC	CC	ENG	SR	KMT	TW	TC
c3000	Yes	80.59	97.93	16.07	0.80	2556	95.7%	30.3	36.0	52.4
	No	79.34	96.72	15.98	0.99	3210	94.2%	30.1	30.7	66.2
c4000	Yes	88.08	107.64	17.95	1.04	3280	76.5%	33.9	48.4	68.5
	No	84.04	102.80	17.13	1.14	3700	72.6%	32.3	39.5	77.3

Table 6. Comparison of the CongestionAware policy with and without ToU energy prices.

Scenario	ToU	PF	TR	TTC	CC	ENG	SR	KMT	TW	TC
c3000	Yes	80.59	97.93	16.07	0.80	2556	95.7%	30.3	36.0	52.4
	No	80.46	97.83	16.08	0.82	2586	95.5%	30.3	33.2	53.4
c4000	Yes	88.08	107.64	17.95	1.04	3280	76.5%	33.9	48.4	68.5
	No	88.00	107.55	17.96	1.03	3250	76.2%	33.9	48.8	68.0

4.3. Sensitivity analysis

In this section, we investigate the impact of different model parameters on the performance of the CongestionAware policy. These parameters include the maximum charging waiting times at a queuing charger, battery capacity, and number of fast and slow chargers in the system.

a. Impact of maximum charging waiting time of vehicles at a queuing charger

The maximum charging waiting time at a queuing charger affects vehicles' availability to serve customers as the operator can delay vehicles' charging operations (idled for serving customers) when estimated queuing time on the assigned charger (has minimum total charging operational time among all chargers) exceeds the maximum threshold. Table 7 compares the performance using 20, 30, 40 minutes and no maximum waiting time limit for different demand scenarios. We can observe that when there is no maximum charging waiting time, the profit is the lowest compared with the other cases, in particular for high-demand scenarios (total charging waiting time is 227.4 hours for no-limit waiting compared with the other cases (less than 70 hours)). This is because the number of fast chargers is very insufficient in the system, and vehicles need to wait a long time at fast chargers if there are no maximum charging time limits. On the other hand, when limiting vehicles' maximum waiting time at a queuing charger, vehicles can be idled to serve customers. Note that when increasing this maximum threshold, the total waiting time increases accordingly. However, the total customer service rate and profit increase if the maximum waiting time threshold is limited, as is the case for a threshold of no more than 40 minutes. In practice, the operator could learn/adjust this threshold based on its day-to-day realized vehicle queuing patterns and charging demands.

Table 7. Impact of maximum waiting time at chargers for the CongestionAware policy.

Scenario	Max. waiting time*	PF	TR	TTC	CC	ENG	SR	KMT	TW	TC
c3000	20	80.49	97.81	16.05	0.79	2527	95.6%	30.3	28.7	50.7
	30	80.59	97.93	16.07	0.80	2556	95.7%	30.3	36.0	52.4
	40	80.82	98.28	16.17	0.81	2586	96.0%	30.5	42.8	55.1

	no limit	80.07	97.48	16.08	0.84	2657	94.9%	30.3	57.1	61.3
c4000	20	87.87	107.28	17.84	1.02	3203	76.1%	33.7	38.6	65.1
	30	88.08	107.64	17.95	1.04	3280	76.5%	33.9	48.4	68.5
	40	88.47	108.21	18.08	1.06	3368	76.7%	34.1	69.4	73.8
	no limit	86.07	105.86	17.73	1.30	4177	74.7%	33.5	227.4	122.1

*: in minutes.

b. Impact of battery capacity

To test the impact of battery capacity, we consider three battery sizes, i.e. 62, 72, and 82 kWh. We consider only the high demand scenario of 4000 customers with identical parameter settings (results for c3000 scenario would draw similar conclusions). Table 8 compares the performance of different charging policies. As expected, increasing the battery size could significantly increase customers' service rate and the system's profit (i.e. customers' service rate increases around 10% for different charging policies if the battery size is increased from 62kWh to 82 kWh). Compared with the benchmark policies, the CongestionAware policy has higher profits and service rates for all battery sizes. When comparing with the second-best benchmark policy (DynaThreshold), the profit and customer service rate increases from 8.77% to 17.03% and from 7.9% to 15.1%, respectively. The results demonstrate that by increasing the battery size (given the same charging station capacity limit), the CongestionAware policy outperforms further the benchmark. This is because when battery size (capacity) increases, vehicles' charging times and waiting times become longer, which could increasingly harm vehicles' availability when charging to 80% for each charging operation. However, the CongestionAware policy devises a smarter charging plan that anticipates vehicles' charging waiting times and energy needs and adapts it (reactive model) to minimize total system costs, resulting in more effective utilization of congested charging facilities.

Table 8. Impact of battery capacity on the KPI using different charging policies (c4000 scenario).

Battery	Charging policy	PF	TR	TTC	CC	ENG	SR	KMT	TW	TC
62 kWh	Nearest	76.55	93.12	15.54	0.82	2657	64.2%	29.3	136.1	93.1
	Fastest	77.31	94.07	15.69	0.84	2745	64.8%	29.6	100.4	93.0
	MinChgOpT	77.56	94.37	15.75	0.85	2796	65.1%	29.7	99.2	93.0
	DynaThreshold	80.98	99.41	16.62	1.15	3751	68.6%	31.4	135.7	120.3
	CongestionAware	88.08	107.64	17.95	1.04	3280	76.5%	33.9	48.4	68.5
72 kWh	Nearest	80.89	98.33	16.42	0.83	2595	68.5%	31.0	127.8	89.0
	Fastest	81.09	98.66	16.48	0.86	2725	68.8%	31.1	122.8	89.1
	MinChgOpT	81.87	99.63	16.65	0.90	2866	69.6%	31.4	120.3	91.7
	DynaThreshold	85.07	104.01	17.39	1.07	3469	72.6%	32.8	116.3	111.7
	CongestionAware	94.30	114.94	19.22	0.94	2954	82.3%	36.3	40.3	59.5
82 kWh	Nearest	84.66	102.77	17.16	0.75	2315	72.4%	32.4	121.8	77.9
	Fastest	84.95	103.19	17.24	0.79	2450	72.6%	32.5	119.7	78.5
	MinChgOpT	85.40	103.74	17.33	0.81	2508	73.1%	32.7	117.3	79.7
	DynaThreshold	85.89	104.66	17.50	0.89	2812	73.5%	33.0	124.7	88.9
	CongestionAware	100.52	122.46	20.56	0.88	2760	88.6%	38.8	34.5	57.5

c. Impact of the number of fast and slower chargers

We further analyze the sensitivity of increasing the number of fast and slower chargers in the system for c3000 (Table 9) and c4000 (Table 10) scenarios. The number of fast and slow chargers is increased from 12 chargers (6 fast and 6 slow) to 20 (10 fast and 10 slow) on the same charging stations (i.e. from 3 fast/slow chargers to 5 fast/slow chargers per charging station). The battery size is 62kWh and the other parameters are identical as described in Section 4.1. For the c3000 scenario, increasing the number of

chargers in the system does reduce the charging congestion for the benchmark policies. The profit, service rate, and charged amount of energy increase along with more fast and slow chargers in the system. The service rate increases around 3% if the number of chargers is increased from 12 to 20. For the CongestionAware policy, the benefit is less significant in terms of customer service rate and total system profit although the total charging waiting time decreases accordingly when the number of chargers increases. For the c4000 scenario, using the benchmark policies results in a significant reduction in total (charging) waiting time (see TW column in Table 10) when increasing the number of chargers from 12 to 16 (i.e. from -31% to -58%). Adding more chargers from 16 to 20 chargers does further reduce total waiting time but is less effective (i.e. from 18% to -44%). The profit (+3.3 to +7.7%) and service rate (+2.1 to +6.2%) increase accordingly due to total waiting time reduction when the number of chargers increases from 12 to 20. For the CongestionAware policy, the effectiveness of increasing the number of chargers becomes much more significant than the benchmark. The profit and service rate are increased by 11.1% (from 88.08k to 97.81k) and 9.8% (from 76.5% to 86.3%), respectively if the number of chargers is changed from 12 to 20. Increasingly, we observe that total charging time is reduced slightly from 48.4 hours (12 chargers) to 43.5 hours (20 chargers), but the total charged amount of energy is increased significantly from 3280kWh to 4467 kWh (+36.2%). In practice, the operator can further invest in their charging infrastructure to increase the system's profitability.

Table 9. System performance for different numbers of fast and slow chargers (c3000 scenario).

# of chargers	Charging policy	PF	TR	TTC	CC	ENG	SR	KMT	TW	TC
12	Nearest	73.02	88.93	14.72	0.89	2824	84.9%	27.8	111.7	94.1
	Fastest	73.46	89.52	14.83	0.92	2935	85.7%	28.0	94.0	94.1
	MinChgOpT	74.45	90.67	15.02	0.94	3011	86.9%	28.3	77.1	92.6
	DynaThreshold	75.08	92.06	15.31	1.06	3430	88.7%	28.9	97.2	107.8
	CongestionAware	80.59	97.93	16.07	0.80	2556	95.7%	30.3	36.0	52.4
16	Nearest	74.82	91.24	15.13	1.02	3264	87.6%	28.5	68.4	113.3
	Fastest	75.63	92.24	15.28	1.03	3298	88.7%	28.8	46.2	106.6
	MinChgOpT	76.69	93.56	15.52	1.09	3516	90.3%	29.3	31.6	105.8
	DynaThreshold	76.55	93.99	15.61	1.24	4016	90.8%	29.5	54.8	126.2
	CongestionAware	80.35	97.66	16.09	0.82	2579	95.3%	30.4	20.9	51.9
20	Nearest	75.60	92.18	15.28	1.03	3283	88.6%	28.8	43.8	120.7
	Fastest	76.39	93.19	15.44	1.06	3414	89.9%	29.1	28.5	111.3
	MinChgOpT	77.73	94.87	15.72	1.15	3756	91.8%	29.7	19.6	106.5
	DynaThreshold	77.26	95.00	15.77	1.38	4443	92.0%	29.8	36.1	141.3
	CongestionAware	80.66	98.03	16.12	0.84	2616	95.7%	30.4	10.1	52.5

Table 10. System performance for different numbers of fast and slow chargers (c4000 scenario).

# of chargers	Charging policy	PF	TR	TTC	CC	ENG	SR	KMT	TW	TC
12	Nearest	76.55	93.12	15.54	0.82	2657	64.2%	29.3	136.1	93.1
	Fastest	77.31	94.07	15.69	0.84	2745	64.8%	29.6	100.4	93.0
	MinChgOpT	77.56	94.37	15.75	0.85	2796	65.1%	29.7	99.2	93.0
	DynaThreshold	80.98	99.41	16.62	1.15	3751	68.6%	31.4	135.7	120.3
	CongestionAware	88.08	107.64	17.95	1.04	3280	76.5%	33.9	48.4	68.5
16	Nearest	78.26	95.17	15.89	0.82	2752	65.6%	30.0	85.5	103.0
	Fastest	79.38	96.62	16.14	0.88	2953	66.6%	30.5	69.7	103.8
	MinChgOpT	80.74	98.30	16.42	0.93	3126	67.9%	31.0	41.8	101.6
	DynaThreshold	84.98	104.25	17.44	1.25	4151	72.4%	32.9	74.8	137.5
	CongestionAware	92.46	113.15	18.92	1.20	3753	80.6%	35.7	45.3	75.4

20	Nearest	79.08	96.15	16.05	0.83	2796	66.3%	30.3	70.3	112.2
	Fastest	80.35	97.82	16.35	0.90	3038	67.6%	30.8	45.3	106.6
	MinChgOpT	81.66	99.35	16.59	0.92	3138	68.7%	31.3	23.6	104.7
	DynaThreshold	87.23	107.02	17.92	1.30	4366	74.8%	33.8	43.0	145.8
	CongestionAware	97.81	120.01	20.07	1.43	4467	86.3%	37.9	43.5	89.9

Note that the day-ahead charging plan model P2 can be solved efficiently using a commercial solver to obtain good approximate solutions given a reasonable computational time limit when the problem size is not too large. For our computational study, we use a one-hour computational time limit, and the obtained solutions have the gaps to the lower bound from around 10% to 14% for the c3000 scenario and around 5% for the c4000 scenario. When the problem size (in terms of the number of customers, vehicles, and fast/slow chargers) increases, we can reduce the computational time by decomposing it into smaller problem-size blocks with proportional customer demand, number of vehicles, and number of chargers in the system to obtain a charging plan for the vehicles of the block and replicate it for the vehicles of the others blocks. Another option is developing efficient heuristics to get good solutions, which remains a future research avenue of this study.

5. Conclusion and discussions

In this study, we develop an effective dynamic charging approach to coordinate vehicle dispatching and charging operations for electric ride-hailing systems under stochastic demand, variable energy prices, and congested charging stations. We focus on maximizing the total system profit by anticipating vehicles' energy needs and waiting time for charging on different chargers during the day to reduce vehicle unavailability and increase the service rate of customers. The proposed sequential MILP approach first determine charging time and target SoCs of vehicles for a long planning horizon based on which a online reactive model optimizes vehicle-to-charger assignment for a short planning horizon to minimize total charging operational costs given current system state. This reactive model adjusts vehicles' charging time and target SoCs after recharge based on vehicle's energy needs and waiting time on chargers for more effective utilization of congested charging stations. Four benchmark charging policies are used to compare the performance of the proposed method: Nearest, Fastest, Minimum charging operational time, and dynamic hourly charging thresholds. We propose more realistic vehicles' queuing modeling at charging stations, i.e., no charging overlaps on each charger and maximum waiting time limits in a queuing charger. A more realistic minimum charging time requirement per charging operation is considered in this study. To the best of our knowledge, it is still neglected in existing studies.

We conducted a simulation case study using NYC yellow taxi data in a Manhattan-like area with two demand scenarios using a fleet of 100 EVs and limited fast and slow charging stations. The computational results show that the developed methodology outperforms the benchmark approaches in terms of higher profit and customer service rates under different scenarios. Overall, compared with the benchmark, the proposed approach increases total profit by 7.65%-10.69% for the scenario of 3000 customers per day and 8.76%-15.05% for that of 4000 customers per day. Similarly, the customer service rate is increased by +7%-10.8% and +7.9%-12.3% for the c3000 and c4000 scenarios, respectively. When increasing the battery size of vehicles and the number of chargers in the system, the service rate could be further improved from 76.5% (12 chargers and 62kWh battery of vehicles) to 88.6% (12 chargers and 82kWh battery) and 86.3% (20 chargers and 62kWh battery) for the CongestionAware policy. Compared with the benchmark, the CongestionAware policy increases the service rate systematically (up to +15.1%-16.2% for the c4000 scenario with 12 chargers and 82kWh battery). Moreover, the total charging waiting time is significantly reduced compared with the benchmark. The proposed approach can be applied to support transport network companies for more efficient charging operation management under limited (congested) charging facilities under demand uncertainty.

Future extensions include developing efficient solution approaches for scaling up the system, applying this approach for optimizing vehicle battery configuration, fleet size and charging infrastructure planning etc. Other interesting research avenues include integrating smart charging strategies to mitigate

the impact of charging operations on the power grid during peak hours or extending this approach for different systems, e.g. shared mobility systems or regular bus services.

Acknowledgments

The work was supported by the Luxembourg National Research Fund (C20/SC/14703944).

References

- Abdullah, H.M., Gastli, A., Ben-Brahim, L., 2021. Reinforcement Learning Based EV Charging Management Systems-A Review. *IEEE Access* 9, 41506–41531. <https://doi.org/10.1109/ACCESS.2021.3064354>
- Ahadi, R., Ketter, W., Collins, J., Daina, N., 2023. Cooperative Learning for Smart Charging of Shared Autonomous Vehicle Fleets. *Transp. Sci.* 57, 613–630. <https://doi.org/10.1287/trsc.2022.1187>
- Al-Kanj, L., Nascimento, J., Powell, W.B., 2020. Approximate dynamic programming for planning a ride-hailing system using autonomous fleets of electric vehicles. *Eur. J. Oper. Res.* 284, 1088–1106. <https://doi.org/10.1016/j.ejor.2020.01.033>
- Bischoff, J., Maciejewski, M., 2014. Agent-based simulation of electric taxicab fleets. *Transp. Res. Procedia* 4, 191–198. <https://doi.org/10.1016/j.trpro.2014.11.015>
- Dean, M.D., Gurumurthy, K.M., de Souza, F., Auld, J., Kockelman, K.M., 2022. Synergies between repositioning and charging strategies for shared autonomous electric vehicle fleets. *Transp. Res. Part D Transp. Environ.* 108, 103314. <https://doi.org/10.1016/j.trd.2022.103314>
- Farazi, P.N., Zou, B., Ahamed, T., Barua, L., 2021. Deep reinforcement learning in transportation research: A review. *Transp. Res. Interdiscip. Perspect.* 11, 100425. <https://doi.org/10.1016/j.trip.2021.100425>
- Froger, A., Mendoza, J.E., Jabali, O., Laporte, G., 2019. Improved formulations and algorithmic components for the electric vehicle routing problem with nonlinear charging functions. *Comput. Oper. Res.* 104, 256–294. <https://doi.org/10.1016/j.cor.2018.12.013>
- Iacobucci, R., McLellan, B., Tezuka, T., 2019. Optimization of shared autonomous electric vehicles operations with charge scheduling and vehicle-to-grid. *Transp. Res. Part C Emerg. Technol.* 100, 34–52. <https://doi.org/10.1016/j.trc.2019.01.011>
- Jamshidi, H., Correia, G.H.A., van Essen, J.T., Nökel, K., 2021. Dynamic planning for simultaneous recharging and relocation of shared electric taxis: A sequential MILP approach. *Transp. Res. Part C Emerg. Technol.* 125. <https://doi.org/10.1016/j.trc.2020.102933>
- Jenn, A., 2019. Electrifying Ride-sharing: Transitioning to a Cleaner Future [WWW Document]. UC Davis Natl. Cent. Sustain. Transp. URL <https://escholarship.org/uc/item/12s554kd> (accessed 12.8.21).
- Kullman, N.D., Cousineau, M., Goodson, J.C., Mendoza, J.E., 2021. Dynamic Ride-Hailing with Electric Vehicles. *Transp. Sci.* 56, 775–794. <https://doi.org/10.1287/trsc.2021.1042>
- Ma, T.-Y., 2021. Two-stage battery recharge scheduling and vehicle-charger assignment policy for dynamic electric dial-a-ride services. *PLoS One* 16, e0251582. <https://doi.org/10.1371/journal.pone.0251582>
- Ma, T.-Y., Xie, S., 2021. Optimal fast charging station locations for electric ridesharing with vehicle-charging station assignment. *Transp. Res. Part D Transp. Environ.* 90, 102682. <https://doi.org/10.1016/j.trd.2020.102682>
- Pantelidis, T.P., Li, L., Ma, T.-Y., Chow, J.Y.J.J., Jabari, S.E.G., 2022. A Node-Charge Graph-Based Online Carshare Rebalancing Policy with Capacitated Electric Charging. *Transp. Sci.* 56, 654–676. <https://doi.org/10.1287/trsc.2021.1058>
- Shi, J., Gao, Y., Wang, W., Yu, N., Ioannou, P.A., 2020. Operating Electric Vehicle Fleet for Ride-Hailing Services with Reinforcement Learning. *IEEE Trans. Intell. Transp. Syst.* 21, 4822–4834. <https://doi.org/10.1109/TITS.2019.2947408>
- Taxi & Limousine Commission, 2022. CHARGED UP! TLC’s Roadmap to Electrifying the For-Hire Transportation Sector in New York City. [https://doi.org/10.12968/S0261-2097\(22\)60151-5](https://doi.org/10.12968/S0261-2097(22)60151-5)
- Yan, P., Yu, K., Chao, X., Chen, Z., 2023. An online reinforcement learning approach to charging and

- order-dispatching optimization for an e-hailing electric vehicle fleet. *Eur. J. Oper. Res.* 310, 1218–1233. <https://doi.org/10.1016/j.ejor.2023.03.039>
- Yang, Z., Guo, T., You, P., Hou, Y., Qin, S.J., 2019. Distributed approach for temporal-spatial charging coordination of plug-in electric taxi fleet. *IEEE Trans. Ind. Informatics* 15, 3185–3195. <https://doi.org/10.1109/TII.2018.2879515>
- Yi, Z., Smart, J., 2021. A framework for integrated dispatching and charging management of an autonomous electric vehicle ride-hailing fleet. *Transp. Res. Part D Transp. Environ.* 95, 102822. <https://doi.org/10.1016/j.trd.2021.102822>
- Zalesak, M., Samaranayake, S., 2021. Real time operation of high-capacity electric vehicle ridesharing fleets. *Transp. Res. Part C Emerg. Technol.* 133, 103413. <https://doi.org/10.1016/j.trc.2021.103413>
- Zhang, R., Rossi, F., Pavone, M., 2016. Model predictive control of autonomous mobility-on-demand systems, in: 2016 IEEE International Conference on Robotics and Automation (ICRA). IEEE, pp. 1382–1389. <https://doi.org/10.1109/ICRA.2016.7487272>

Appendix A. Comparison of different modeling approaches for vehicle queuing at chargers for the benchmark charging policies.

In the literature, existing studies assume a simplified vehicle queuing behavior modeling at chargers/charging stations, i.e., vehicles wait in a queued charger/charging station for charging without time limits. This might not be realistic when the vehicle's queuing times are very long (e.g., several hours). In this case, drivers (vehicles) might prefer to move to other nearby chargers or least-waiting-time chargers to recharge and return to serve customers earlier. To investigate the impact of queuing behavior at chargers, three modeling approaches are tested as follows. Note that vehicles' charger assignments are determined by the applied charging policies.

- a. **Naïve queuing:** Vehicles wait in a queue for their target(assigned) charger without a time limit.
- b. **Charger-chasing A:** Vehicles wait at a charger (current charger) with a maximum waiting time of 15 minutes, then move away to a fast charger (next charger) with the least waiting time when arriving at chargers' locations. If vehicles cannot reach the next charger due to insufficient SoCs, vehicles go to the closest charger to recharge. If unable to reach the closest one, vehicles wait at the current charger until its turn.
- c. **Charger-chasing B:** Different from charger-chasing A, vehicles go to a fast or slow charger with the least waiting time when moving away from the queue on current chargers.

Table A1 reports the performance of using different vehicle queuing modeling approaches. The upper block in Table A1 is related to the c3000 scenario, while the lower block to the c4000 scenario. The results show that using charger-chasing B has the highest service rates and profits for both demand scenarios. The total waiting time at chargers using charger-chasing B is systematically lower than that of charger-chasing A. However, using the naïve queue approach does not necessarily make it worse in terms of total waiting time compared to the charger-chasing approach. It may depend on the applied charging policy and uncertain queuing situations at chargers.

We further look into the details of the realized charging sessions for the c3000 scenario (The c4000 scenario has similar results; we neglect it here). Table A2 shows the results of using different queuing modeling approaches for the benchmark charging policies for the c3000 scenario. When using the naïve queuing approach, the number of realized charging operations is significantly fewer than the charger-chasing approaches due to the long waiting time on queued chargers. The charger-chasing B has the lowest average queuing time at chargers per charging session (5.55 minutes compared with the charger-chasing A (6.15 minutes) and the naïve queuing (106.4 minutes)). The average charged amount of energy is similar. Still, the average charging times of charger-chasing B are higher than the charger-chasing B as the latter considers both fast and slow chargers when vehicles go away from the current charger, resulting in more utilization of slow chargers to charge from vehicles' current SoC to E_v^{max} . Figure A1 reports the boxplots for vehicle queuing time at chargers for realized charging sessions for the naïve queue and the charger-chasing B. It shows that using the naïve queue approach might result in an unrealistic long queuing time for a charger while using the charger-chasing B would not have this issue.

Table A2. Effect of different modeling approaches for vehicle queuing at chargers.

Scenario	Queuing approach	Charging policy	PF	TR	TTC	CC	ENG	SR	KMT	TW	TC	
c3000	Naïve queuing	Nearest	65.11	78.43	12.94	0.33	1049	74.1%	24.4	80.5	34.7	
		Fastest	73.00	88.69	14.70	0.81	2603	84.8%	27.7	109.2	62.6	
		MinChgOpT	74.16	90.16	14.94	0.86	2775	86.4%	28.2	87.9	66.4	
		DynaThreshold	74.92	91.27	15.15	0.91	2955	87.7%	28.6	120.5	67.0	
	Charger-chasing A	Nearest	73.02	88.93	14.72	0.89	2824	84.9%	27.8	111.7	94.1	
		Fastest	73.11	89.07	14.77	0.86	2774	85.1%	27.9	125.2	73.1	
		MinChgOpT	73.89	89.95	14.90	0.87	2807	86.2%	28.1	103.8	70.6	
		DynaThreshold	74.28	90.99	15.11	0.96	3112	87.4%	28.5	137.8	71.3	
	Charger-chasing B	Nearest	73.02	88.93	14.72	0.89	2824	84.9%	27.8	111.7	94.1	
		Fastest	73.46	89.52	14.83	0.92	2935	85.7%	28.0	94.0	94.1	
		MinChgOpT	74.45	90.67	15.02	0.94	3011	86.9%	28.3	77.1	92.6	
		DynaThreshold	75.08	92.06	15.31	1.06	3430	88.7%	28.9	97.2	107.8	
	c4000	Naïve queuing	Nearest	65.96	79.63	13.26	0.36	1160	55.4%	25.0	96.7	37.6
			Fastest	76.34	92.83	15.50	0.81	2641	64.0%	29.2	122.1	63.9
			MinChgOpT	77.83	94.63	15.80	0.84	2714	65.2%	29.8	87.0	69.5
			DynaThreshold	80.45	98.25	16.44	1.04	3390	67.8%	31.0	182.7	80.5
Charger-chasing A		Nearest	76.55	93.12	15.54	0.82	2657	64.2%	29.3	136.1	93.1	
		Fastest	76.07	92.55	15.44	0.81	2643	63.8%	29.1	138.3	73.2	
		MinChgOpT	77.01	93.69	15.63	0.84	2740	64.7%	29.5	126.3	74.0	
		DynaThreshold	78.92	96.99	16.22	1.09	3564	66.7%	30.6	170.3	89.9	
Charger-chasing B		Nearest	76.55	93.12	15.54	0.82	2657	64.2%	29.3	136.1	93.1	
		Fastest	77.31	94.07	15.69	0.84	2745	64.8%	29.6	100.4	93.0	
		MinChgOpT	77.56	94.37	15.75	0.85	2796	65.1%	29.7	99.2	93.0	
		DynaThreshold	80.98	99.41	16.62	1.15	3751	68.6%	31.4	135.7	120.3	

Table A2. Statistics of realized charging sessions for different modeling approaches for vehicle queuing at chargers (c3000 scenario).

Queuing approach	Charging policy	# of realized charging sessions	Average queuing times per charging session	Average charging times per charging session	Average charged energy per charging session
Naïve queuing	Nearest	26	165.9	81.0	38.8
	Fastest	68	96.3	59.5	40.3
	MinChgOpT	72	77.0	58.4	39.9
	DynaThreshold	84	86.4	49.5	36.0
Charger-chasing A	Nearest	71	5.9	80.8	39.4
	Fastest	74	6.2	64.6	39.4
	MinChgOpT	69	6.0	60.9	41.0
	DynaThreshold	87	6.5	48.9	36.6
Charger-chasing B	Nearest	71	5.9	80.8	39.4
	Fastest	76	4.8	75.8	39.9
	MinChgOpT	80	5.5	73.6	39.6
	DynaThreshold	98	6.0	67.4	36.6

Remark: Time is measured in minutes; energy is measured in KWh.

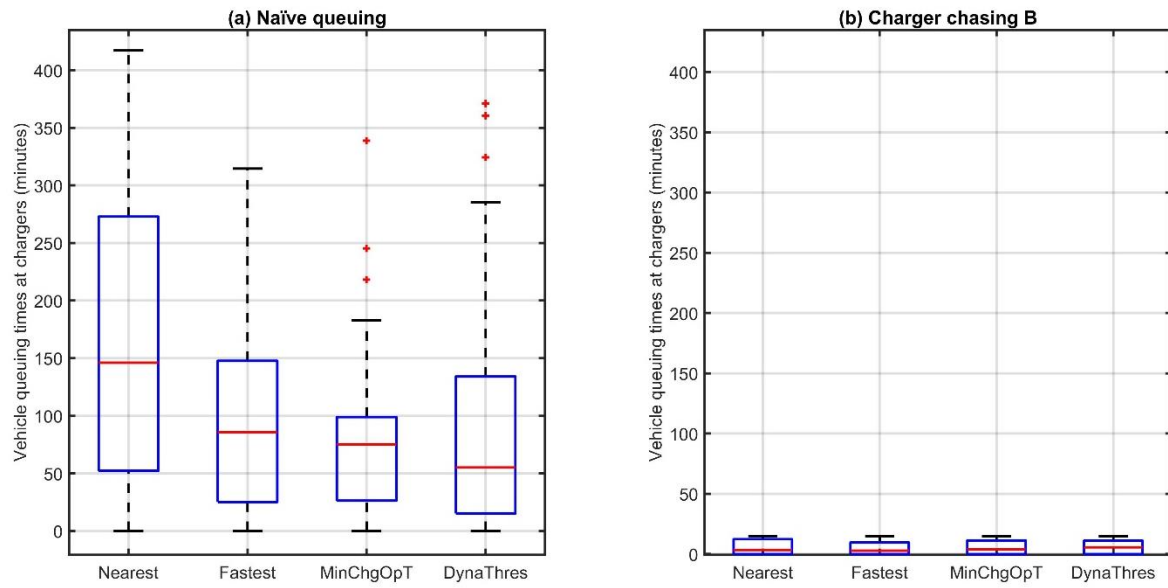


Figure A1. Boxplots for vehicle queuing times at chargers of the realized charging sessions for the benchmark charging policies. Naïve queueing (on the left) and charger-chasing B (on the right).